Quantum computation without strict strong coupling on a silicon chip

Yun-Feng Xiao,* Zheng-Fu Han,† and Guang-Can Guo‡
Key Laboratory of Quantum Information, University of Science and Technology of China, Hefei 230026, People's Republic of China
(Received 19 September 2005; published 31 May 2006)

We propose a potential quantum-computer hardware-architecture model on a silicon chip in which the basic cell gate is the atom-photon controlled-phase-flip gate. This gate can be implemented through a single-photon pulse's scattering by a toroidal microcavity trapping a neutral atom, and it does not require very strict strong-coupling regime and can work beyond the Lamb-Dicke limit with high fidelity and success probability under practical noise environments. Especially, *good* and *bad* losses of the toroidal cavity are discussed in detail. Finally, a possibly simple experiment based on current experimental technology is proposed to demonstrate our scheme.

DOI: 10.1103/PhysRevA.73.052324 PACS number(s): 03.67.Lx, 42.50.Pq, 42.60.Da, 42.82.Et

I. INTRODUCTION

A number of theoretical and experimental schemes have been proposed to perform the quantum computation and build a quantum computer. To realize universal quantum computation, one of the biggest obstacles is the quantum hardware which plays a central role in the future quantum computer. The proposals based on atomic, molecular, and optical physics, solid state, and linear optics, etc., have been suggested to construct a quantum computer [1] over the past few years. Here, we focus on cavity-QED-based quantum computation [2,3], especially, distributed quantum computation [4,5]. Such proposals are very promising and highly inventive. However, scalable quantum gates are especially demanded for large-scale quantum computation.

Earlier approaches have turned out to be very challenging owing to many technique difficulties, for example, the ability to link spatially distant cavities with optical fibers. For Fabry-Perot (FP) cavity which is widely discussed currently, optical fiber coupling is possible. However the total coupling efficiency is limited due to the absorption of cavity mirrors [6]. Mirror absorption occupies an innegligible proportion in the total cavity dissipation. Currently, the absorptive loss and the transmission rate of the mirror coating are about 3.0 ppm and 4.5 ppm, respectively [6]. It is difficult to gain smaller absorption and freely control transmission grounded on current mirror coating, polishing and coupling technologies. For photonic crystal defect cavity which is another currently considered candidate, the demonstrated efficiency is only about 44% [7]. Therefore, in order to build a future large-scale quantum computer through cavity QED, it is an important task to look for another optical cavity system which not only possesses high optical quality but also owns inherent capability.

Motivated by the pioneering work of Braginsky and Ilchenko [8], some of the high quality optical cavities to date have been achieved in the form of whispering gallery mode (WGM), such as microcylinders, microdisks, and microspheres [9]. The combination of their ultrahigh quality factor Q, very small mode volume V_m, and relatively easy fabrication process, drives them as promising candidates besides FP cavities for cavity QED experiments [10,11]. Recently, toroidal microcavity, a new type of WGM-based optical cavity was fabricated by a combination of standard lithography, dry etching technique, and selective reflow process, as outlined in Ref. [12]. This kind of resonator has the following advantages: (i) It supports very few radial and azimuthal modes, and it is in contrast to microspheres which support $(2l+1)$ azimuthal modes. So this cavity system is allowed for single-mode operations in principle. (ii) It has ultrahigh Q factor which has been demonstrated up to 4×10^8 [13], and smaller mode volumes compared with microsphere cavity. Routinely, V_m is less than 100 μm^3 for regular minor and principal diameters [12,13], which indicates that there is an ultrahigh coherent coupling factor $g(r)=(\mu^2\omega_c/2\hbar\varepsilon_0 V_m)^{1/2}$ between an individual atom and a WGM field of interest. (iii) The shape of toroidal microcavity allows an extra level of geometric control over that provided by a spherical microcavity [12], leading to high experiment repeatability and controllable cavity modes. And more important, with the assistance of taper waveguides, toroidal microcavity allows ultrapowerful integration on a silicon chip which enhances the physical capability and thus offers a possibility of high-performance quantum network.

II. TWO-SIDE-CAVITY MODEL

In this paper, we describe a potentially applicable hardware model for scalable distributed quantum computation and quantum networks based on toroidal microcavities and waveguides in which the key step is to implement the atom-photon quantum controlled-phase-flip (CPF) gate. To build this model, we consider a neutral atom (for instance, cesium which is discussed in Ref. [13]) located near the microtoroid surface [14], interacting with a fundamental TM cavity mode since it holds the highest Q and the smallest V_m. For a *bare* toroidal cavity, it is too hard to be used in cavity QED experiments because of its full symmetry. WG modes in the cavity cannot be excited and collected efficiently in free space. Therefore, two taper waveguides are introduced as controlled input and output ports of the cavity, as sketched in

*Electronic address: yfxiao@mail.ustc.edu.cn
†Electronic address: zfhan@ustc.edu.cn
‡Electronic address: gcguo@ustc.edu.cn

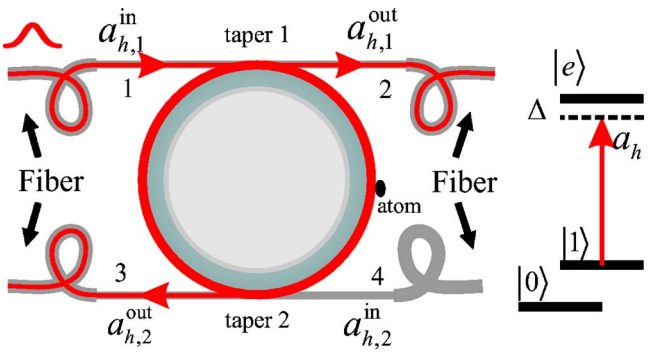

FIG. 1. (Color online) Left-hand side: Coupling between two taper waveguides and a microtoroid. The h component of single-photon pulse resonantly couples into the bare cavity via waveguide 1 (port 1) and departs through waveguide 2 (port 3), while in any other case, it directly passes the waveguide 1 and then leaves from the cavity via port 2. Right-hand side: The energy level diagram of the trapped atom, and transition $|1\rangle \rightarrow |e\rangle$ (for example, the D2 transition of cesium), with h polarization, couples to the cavity mode.

Fig. 1. The Hamiltonian for the single atom and single cavity mode (h polarized) has the form $H=\Delta|e\rangle\langle e|+[g(r)a_h^\dagger\sigma_- + \mathrm{H.c.}]$ in the rotating frame at the cavity frequency ω_c (in units of $\hbar=1$), where $a_h^\dagger$ represents the creation Bose operator for h-polarized cavity photons; σ_- denotes atomic descending operator $|1\rangle\langle e|$; Δ is defined as energy difference $(\omega_e-\omega_c)$ between the atomic transition $|1\rangle \rightarrow |e\rangle$ and cavity mode; H.c. stands for the Hermitian conjugate.

For the toroidal cavity described above in the absence of the atom, it includes three decay paths: two input-output ports with associated loss coefficients κ_1 and κ_2 which can be considered as *good loss*, the intrinsic decay of the bare cavity mode itself described by κ_0 which is the *bad loss*. We also define the total dissipation of the cavity mode $\kappa=\kappa_0+\kappa_1+\kappa_2$ for convenience. In addition, the decay of the bare cavity mode and the atom are described by Lindblad relaxation operators $\mathcal{L}_c=\sqrt{\kappa_0}a_h$ and $\mathcal{L}_a=\sqrt{\gamma_s}|1\rangle\langle e|$, respectively; here γ_s denotes the atomic spontaneous rate of the state $|e\rangle$ to the ground state $|1\rangle$. We neglect the spontaneous loss of the upper level to other states. Therefore, omitting the terms which concern the Langevin noises that have negligible contribution to the dynamics, we can easily obtain Heisenberg equations of motion for the internal cavity field and the atom,

$$\frac{da_h(t)}{dt} = -i[a_h,H] - \frac{\kappa_0}{2}a_h(t) - \sum_{j=1,2}\left(\frac{\kappa_j}{2}a_h(t) + \sqrt{\kappa_j}a_{h,j}^{in}(t)\right), \tag{1a}$$

$$\frac{d\sigma_-(t)}{dt} = -i[\sigma_-,H] - \frac{\gamma_s}{2}\sigma_-(t), \tag{1b}$$

$$\frac{d\sigma_z(t)}{dt} = -i[\sigma_z,H] - 2\gamma_s\sigma_{ee}(t), \tag{1c}$$

where the atomic operator σ_z (σ_{ee}) is defined as $|e\rangle\langle e|-|1\rangle\times\langle 1|$ ($|e\rangle\langle e|$), and there are commutation relations $[a_h(t),a_h^\dagger(t)]=1$ for the cavity mode field and $[a_{h,j}^{in}(t),a_{h,j}^{in\dagger}(t')]=\delta(t-t')$ for the one-dimensional input h-polarized single-photon optical field. By taking the Fourier transform $A(\omega)=\frac{1}{\sqrt{2\pi}}\int A(t)e^{i\omega t}dt$, we have [15–17]

$$a_h(\omega) = \frac{g(r)\sigma_-(\omega) - i\sum_{j=1,2}\sqrt{\kappa_j}a_{h,j}^{in}(\omega)}{\omega + \frac{i\kappa}{2}}, \tag{2a}$$

$$\sigma_-(\omega) = \frac{-g^*(r)}{\omega-\Delta+\frac{i\gamma_s}{2}}\frac{1}{\sqrt{2\pi}}\int \sigma_z(\omega-\omega')a_h(\omega)d\omega', \tag{2b}$$

$$\sigma_z(\omega) = \frac{1}{\omega+i\gamma_s}\left(-i\gamma_s P(\omega) - \sqrt{\frac{2}{\pi}}\int g(r)\sigma_-(\omega-\omega')\times a_h^\dagger(\omega)d\omega' - \mathrm{H.c.}\right), \tag{2c}$$

where we have introduced the projector operator $P=|e\rangle\langle e|+|1\rangle\langle 1|$ which counts the probability that the atom perches in the state space $\{|1\rangle,|e\rangle\}$, and $P(\omega)$ is its Fourier transform, obviously, $P(\omega)=\delta(\omega)$. It is hard to get an analytical solution of the above equations. However, we can get an expression of $a_h(\omega)$ by omitting the terms involving more than one $a_h(\omega)$ operator since the input field is a sufficiently weak single-photon pulse in our scheme, so we can obtain

$$a_h(\omega) = \frac{-i\sum_j\sqrt{\kappa_j}a_{h,j}^{in}(\omega)}{(\omega-\omega_c)+\frac{i}{2}\kappa-s} \tag{3}$$

in which $s=i|g(r)|^2\gamma_s/(\omega-\Delta+\frac{i}{2}\gamma_s)(\omega+i\gamma_s)$. Meanwhile, the cavity output $a_{h,j}^{out}(\omega)$ is associated with the input by the standard input-output formalism $a_{h,j}^{out}(\omega)=a_{h,j}^{in}(\omega)+\sqrt{\kappa_j}a_h(\omega)$ which expresses the output field as a sum of the input field plus the field radiated from the microtoroid cavity via the waveguide. It is easy to find

$$a_{h,j}^{out}(\omega) = \frac{\left(\omega+\frac{i}{2}(\kappa_0+\kappa_{3-j}-\kappa_j)-s\right)a_{h,j}^{in}(\omega) - i\sqrt{\kappa_1\kappa_2}a_{h,3-j}^{in}(\omega)}{\omega+\frac{i}{2}\kappa-s} \tag{4}$$

We offer some brief remarks to our scheme before we get the ultimately distinct expression $a_{h,j}^{out}(\omega)$. First, the single-photon pulse resonantly couples into the cavity only through the taper 1, so we can execute $a_{h,2}^{in}(\omega)=0$. Second, we need to operate the system in the limit with $\kappa T \gg 1$ in our scheme, which implies the bandwidth ($\propto 1/T$) of the single photon in frequency domain is much narrower than the cavity mode (2κ) and the linewidth ($2\gamma_s$) of the atomic energy level $|e\rangle$, i.e., $|\omega| \ll (\kappa,\gamma_s)$. In particular, near-field coupling constructs efficiently only based on this condition. Finally, we use the relation $\kappa_1=\kappa_0+\kappa_2$ to match the loss of cavity, which means

the coupling to the cavity from the input waveguide (κ_1) compensates for both the intrinsic loss of the cavity (κ_0) and the power coupling to the other waveguide (κ_2). It is more interesting that we have noticed that the result agrees with the condition of criticality $Q_{\text{bus}}^{-1}=Q_{\text{drop}}^{-1}+Q_0^{-1}$ in Ref. [18]. Sum up the above and we can get

$$a_{h,1}^{\text{out}}(\omega)=\frac{-|g(r)|^2/\left(-\Delta+\frac{i}{2}\gamma_s\right)}{\frac{i}{2}\kappa-|g(r)|^2/\left(-\Delta+\frac{i}{2}\gamma_s\right)}a_{h,1}^{\text{in}}(\omega), \tag{5a}$$

$$a_{h,2}^{\text{out}}(\omega)=\frac{-i\sqrt{\kappa_1\kappa_2}}{\frac{i}{2}\kappa-|g(r)|^2/\left(-\Delta+\frac{i}{2}\gamma_s\right)}a_{h,1}^{\text{in}}(\omega). \tag{5b}$$

In order to get the expected results we discuss $a_{h,j}^{\text{out}}(\omega)$ for two different Δ.

(i) If the atomic transition $|1\rangle\rightarrow|e\rangle$ is resonant with the cavity mode of interest, i.e., $\Delta=0$, then Eqs. (5) can be rewritten as

$$a_{h,1}^{\text{out}}(\omega)=\frac{|g(r)|^2}{\frac{1}{4}\kappa\gamma_s+|g(r)|^2}a_{h,1}^{\text{in}}(\omega), \tag{6a}$$

$$a_{h,2}^{\text{out}}(\omega)=-\frac{2\sqrt{\kappa_1\kappa_2}/\kappa}{1+4|g(r)|^2/(\kappa\gamma_s)}a_{h,1}^{\text{in}}(\omega). \tag{6b}$$

With the choice of the condition $|g(r)|^2/\kappa\gamma_s\gg 1$, we find a more abbreviated expression

$$a_{h,1}^{\text{out}}(\omega)\lessapprox a_{h,1}^{\text{in}}(\omega), \text{ and } a_{h,2}^{\text{out}}(\omega)\approx 0. \tag{7}$$

Both equations indicate that the single-photon pulse propagating in the waveguide does not couple into the cavity even though there is a perfect combination of phase matching and modal frequency selection between the waveguide mode and the *bare* cavity mode. The fact can be explained by the dressed mode theory. When passing the coupling junction, the input photon pulse sees two dressed cavity modes derived from resonant atom-cavity coupling, not the original bare cavity mode itself again. The dressed modes are significantly detuned from the input single-photon pulse by $\delta=\pm g(r)$, respectively [19]. In other words, the input single-photon pulse and the cavity (including the atom) dissatisfy the condition of near-field evanescent wave coupling [18]. Therefore, the system (atom+photon) cannot get any global phase in the case of the resonance between the atomic transition and the bare cavity mode.

(ii) If the atomic transition is largely detuned with the cavity mode, or the atom occupies the other ground state $|0\rangle$ which is an assistant state and is largely detuned with the bare cavity mode, as showed in Fig. 1, then Eqs. (5) are expressed as

$$a_{h,1}^{\text{out}}(\omega)\rightarrow 0, \tag{8a}$$

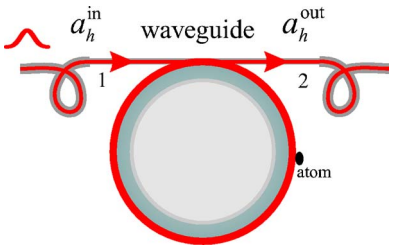

FIG. 2. (Color online) Coupling between a microtoroidal cavity and one taper waveguide. The single-photon pulse inputs from port 1 and outputs from port 2. Only when the atom is in the state $|0\rangle$ and input photon pulse is h polarization, the pulse will couple into and then couples out of the cavity via the same waveguide.

$$a_{h,2}^{\text{out}}(\omega)\rightarrow-\frac{\sqrt{\kappa_1\kappa_2}}{\kappa/2}a_{h,1}^{\text{in}}(\omega), \tag{8b}$$

in this case we have $\Delta\gg|g(r)|,\kappa,\gamma_s$. The result shows that the photon will fully couple into the cavity and then couples to the second waveguide. Most important, the system obtains a global phase $e^{i\pi}$ after the pulse departs from the cavity. Furthermore, the large detuning is equivalent to the case that no atom is in the cavity, in which the transmission $T_{\text{tran}}=0$. And the coupling efficiency from the taper waveguide 1 to 2, $D=\left(-\frac{\sqrt{\kappa_1\kappa_2}}{\kappa/2}\right)^2=1-\frac{2\kappa_0}{\kappa}$, can be obtained from Eqs. (8), and it is also a conclusion in Ref. [18].

By now we can expediently show how to realize an atom-photon CPF gate. We summarize as follows: (i) The photonic (atomic) qubit is initially prepared in an equal (arbitrary) coherent superposition of two orthogonal polarization components (two atomic ground states) and can be expressed as $|\varphi\rangle_p=(|h\rangle+|v\rangle)/\sqrt{2}$ ($|\varphi\rangle_a=\alpha|0\rangle+\beta|1\rangle$). (ii) Guide the single-photon pulse to pass the coupling junction, as displayed in the Fig. 2 and its caption. When the atom rests on the state $|0\rangle$, h component of the single-photon pulse obtains $e^{i\pi}$ global phase change after it departs from the cavity through the port 3, and v component does not gain any phase change because it directly passes the coupling region to the port 2 without any cavity influence; when the atom is in the state $|1\rangle$, both components of the pulse do not gain any phase change because the photon is largely detuned with the dressed cavity modes and passes the cavity directly. As a final result based on above analysis, we have $|\Psi\rangle_{ini}=(\alpha|0\rangle+\beta|1\rangle)(|h\rangle+|v\rangle)/\sqrt{2}\xrightarrow{\text{Ideal CPF}}|\Psi\rangle_{\text{ideal}}=(-\alpha|0\rangle|h\rangle+\alpha|0\rangle|v\rangle+\beta|1\rangle|h\rangle+\beta|1\rangle|v\rangle)/\sqrt{2}$. To obtain atom-atom phase gate one just simply combines several atom-photon phase gates [20].

III. SINGLE-SIDE-CAVITY MODEL IN OVER-COUPLING REGIME

In the above analysis, the scheme works under the regime of critical coupling [18] between the cavity and the taper waveguide 1 due to the loss relationship $\kappa_1=\kappa_0+\kappa_2$. However, it is not easy work to modulate every input waveguide on the chip to achieve the critical-coupling regime and keep the coupling steady going. Fortunately, in the case of the

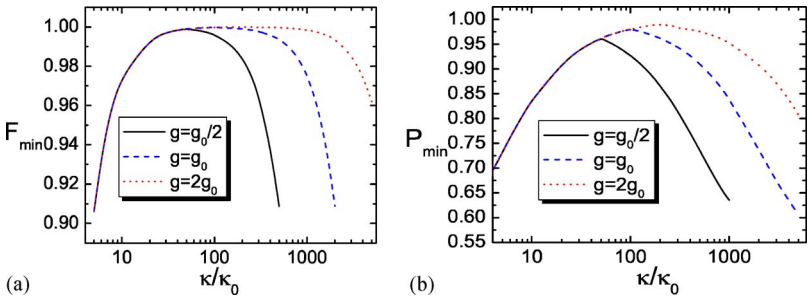

FIG. 3. (Color online) (a) Minimal gate fidelity of the atom-photon phase gate vs κ/κ_0 and single-photon coupling rate g. (b) Minimal success probability of the gate for different κ/κ_0 and g. Other common parameters, $g_0/(2\pi)=86$ MHz, $\kappa_0/(2\pi)=1.4$ MHz, $\gamma_s/(2\pi)=2.6$ MHz, $T=1$ μs.

deep over-coupling regime, the atom-photon CPF gate can also be performed robustly, and the scheme can be even further simplified by removing taper waveguide 2 (see Fig. 2). In this case, taper waveguide 1 is utilized as both input and output ports of the single-photon pulse.

As a theoretical treatment, we just need $\kappa_2=0$ and $a_{h,2}^{\text{in}}(\omega)=0$ in Eqs. (3) and (4). Then Eq. (4) reduces to

$$a_h^{\text{out}}(\omega)=\frac{\omega+\frac{i}{2}(\kappa_0-\kappa_1)-s}{\omega+\frac{i}{2}(\kappa_0+\kappa_1)-s}a_h^{\text{in}}(\omega), \tag{9a}$$

$$a_v^{\text{out}}(\omega)=a_v^{\text{in}}(\omega). \tag{9b}$$

In the limit of $\kappa T\gg 1$, Eqs. (9) can be simplified to the following output-input relations:

$$a_{h,0}^{\text{out}}(\omega)=\frac{\kappa_0-\kappa_1}{\kappa_0+\kappa_1}a_{h,0}^{\text{in}}(\omega), \tag{10a}$$

$$a_{h,1}^{\text{out}}(\omega)=\frac{\frac{i}{2}(\kappa_0-\kappa_1)-s}{\frac{i}{2}(\kappa_0+\kappa_1)-s}a_{h,1}^{\text{in}}(\omega), \tag{10b}$$

$$a_{v,0}^{\text{out}}(\omega)=a_{v,0}^{\text{in}}(\omega), \tag{10c}$$

$$a_{v,1}^{\text{out}}(\omega)=a_{v,1}^{\text{in}}(\omega), \tag{10d}$$

where the subscripts $h(v)$ and 0 (1) denote the input photon polarization and the atomic occupation state, respectively. If $|g(r)|^2/\kappa\gamma_s\gg 1$ and $\kappa_1/\kappa_0\gg 1$ (deep over-coupling case), we get the final expression

$$a_{h,0}^{\text{out}}(\omega)=-a_{h,0}^{\text{in}}(\omega), \tag{11a}$$

$$a_{h,1}^{\text{out}}(\omega)=a_{h,1}^{\text{in}}(\omega), \tag{11b}$$

$$a_{v,0}^{\text{out}}(\omega)=a_{v,0}^{\text{in}}(\omega), \tag{11c}$$

$$a_{v,1}^{\text{out}}(\omega)=a_{v,1}^{\text{in}}(\omega). \tag{11d}$$

This indicates that atom-photon phase gate can be performed in the over-coupling limit. At this time, other than FP cavity, a toroid represents a *natural* single-side cavity which can reduce the gate operation difficulty. In the following, we can find the present scheme works robustly in a large range of κ_1 which also decreases the experimental difficulty.

IV. GATE FIDELITY AND SUCCESS PROBABILITY

An efficient measure of the distance between the quantum logic gates is the fidelity which can be defined as $F\equiv|\langle\Psi_{\text{out}}||\Psi_{\text{ideal}}\rangle|^2$ in the present case, where $|\Psi_{\text{out}}\rangle$ is the output state of the atom and photon after the actual CPF gate and $|\Psi_{\text{ideal}}\rangle$ is the ideal output state. Equation (3) first reveals that the fidelity of our scheme depends only on the magnitude of the coupling factor $g(r)$, but not on its phase. Therefore, it is not necessary to trap the atom within one wavelength scale space range and thus our scheme is robust even beyond Lamb-Dicke limit. The same result also can be obtained in the numerical simulation [21,20] and quantum trajectory simulation [22]. In order to obtain the numerical fidelity we directly calculate Eqs. (9) and consider a finite pulse whose profile is described by a Gauss function $f(t)\propto\exp[-(t-T/2)^2/(T/5)^2](t\in[0,T])$ or any other shapes [23] with long pulse duration for realistic application. For the initial system state $(|h\rangle+|v\rangle)/\sqrt{2}\otimes(\alpha|0\rangle+\beta|1\rangle)$, simply we obtain

$$F=\frac{1}{4}\left|\int\left\{|\alpha|^2\left[1-\exp\left(i\arg\frac{a_h^{\text{out}}(\omega)|_{\Delta\to\infty}}{a_h^{\text{in}}(\omega)}\right)\right]+|\beta|^2\left[1+\exp\left(i\arg\frac{a_h^{\text{out}}(\omega)|_{\Delta=0}}{a_h^{\text{in}}(\omega)}\right)\right]\right\}|\mathcal{F}(\omega)|^2d\omega\right|^2, \tag{12}$$

where $\mathcal{F}(\omega)$ is the Fourier spectrum of the pulse. Note we have normalized the factors of the final state since the photon loss just decreases the success probability in our CPF-gate scheme.

As shown in Fig. 3(a), the minimal fidelity F_{min} (for different initial atomic state) reaches very high, and it is up to 0.9998 for a set of parameters $[g_0/(2\pi),\kappa_0/(2\pi),\gamma_s/(2\pi),\kappa/\kappa_0]=(86\text{ MHz},1.4\text{ MHz},2.6\text{ MHz},100)$ given in Ref. [13]. Remarkably, the fidelity keeps high even though the coherent coupling rate g is less than the total cavity decay κ, and thus our scheme can work robustly without strict strong coupling ($g\gg\kappa,\gamma_s$). Obviously, κ/κ_0 and g/κ are two key parameters in the interest of higher gate fidelity. Big κ/κ_0 indicates that *good loss* dominates the cavity dissipation. However, κ cannot be infinitely large for a given single-photon coupling rate g. This can be understood from the dressed-mode theory, that is, δ should be kept on the order of

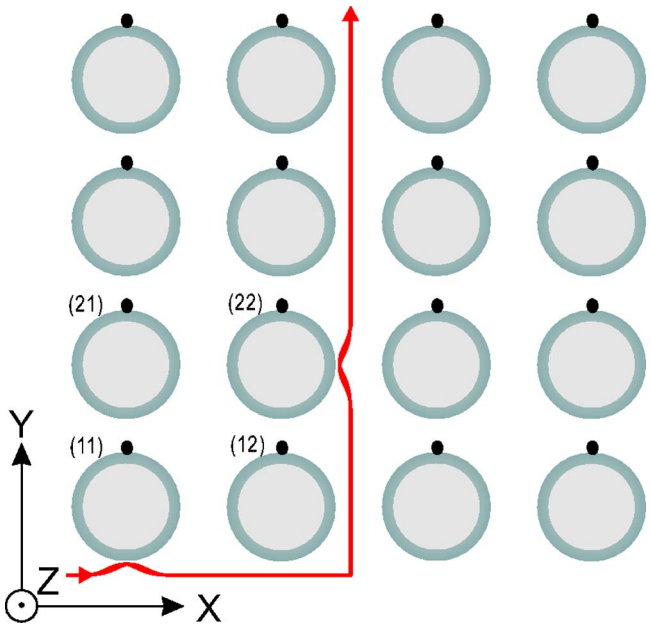

FIG. 4. (Color online) Sketched architecture model of the quantum hardware. The whole system is built on a chip. The waveguides in the figure are working for a realization of CPF gate between atoms (11) and (22).

the cavity mode half-width κ. So decreasing κ_0 is the only best way to obtain large κ/κ_0. WGM-based toroidal cavity has much larger g_0 and smaller κ_0 than the FP cavity, and its κ_0 still has the potential to decrease two magnitudes compared with the current obtained level. Furthermore, using the near-field coupling method described in Ref. [18], one can easily modulate κ_1 through electric control of the distance between waveguides and microtoroid.

Figure 3(b) shows the minimal success probability of the gate which is related with photon loss during gate operation if we detect the output photon. It is easily found that $P_{\min}$ is also dependent on both κ/κ_0 and g/κ. Similar with the fidelity, $P_{\min}$ also has maximum for a given g and an appropriate κ/κ_0, and bigger g results in the higher $P_{\min}$. Both $F_{\min}$ and $P_{\min}$ can be improved by increasing g, reducing κ_0 and optimizing κ/κ_0. However, our scheme still works robustly, with the high gate fidelity and success probability in a large range of κ/κ_0 and g/κ, and thus it decreases the experimental difficulties.

V. QUANTUM HARDWARE MODEL AND GATE OPERATION

Now, we sketch our quantum computer hardware architecture model in Fig. 4 by using above atom-photon CPF gates.

(i) Toroidal cavities, trapping one atom, respectively, can be regularly built on a silicon chip (on the $X-Y$ plane in Fig. 4) in which taper waveguides are used to link arbitrary distant cavities. The trapped atoms represent stationary qubits for their long coherence time of ground inner states and flying photonic qubits allow robust communication between arbitrary nodes of the distributed quantum computation network. With the advance of current semiconductor technology, fiber tapers can even be replaced by demonstrated etched waveguides [24,25]. (ii) The gap between etched waveguides and microcavities can be controlled through the etched electrodes [26] (not described in Fig. 4), which are of importance since they permit designing appropriate quantum circuit to accomplish a given quantum algorithm by simply opening or closing the coupling between waveguides and microcavities. (iii) We built our model by assuming single neutral atoms are trapped near the surface of microcavities using optical lattice [27], which is still relatively difficult under current experimental technology. However, several possible methods may be utilized in the future. For example, single neutral atoms, or possible rare-earth ions may be placed on the toroidal cavity by STM. Using the same theory model, single built quantum dots can work instead of single trapped atoms in the present architecture. Most interesting, coupling in the WGM-based microsphere cavity with single nitrogen-vacancy defect centers was observed recently [28], which is a great advance in WGM-based cavity QED research. Therefore, the whole quantum hardware system, including the etched toroidal silica cavity with the three-level quantum, waveguide, and electrode, has the potential to be produced on a silicon chip.

Now we show how to implement some universal gate operations. First, single-bit rotations on photons can be easily performed through some embedded waveplates which can also be integrated in a chip and controlled by some respective electrodes. Single-bit rotations on three-level quantum (here we assume they are atoms for convenience) can be realized by two classical lasers' irradiation (along Z axis in Fig. 4) which are also used to write in and read out information of the stationary qubits with a very high precision. Second, to perform two-bit operation between two distant atoms, for instance, the atoms (11) and (22) shown in Fig. 4, one only need open the coupling to the respective cavities through their etched electrodes. At this time, other cavities with atoms are beyond the coupling system. A single-photon pulse then interacts with the two cavities in turn, and thus it carries out CPF gate operation between the two distant atoms.

Our hardware model is also especially suitable for the generation of an atomic cluster state of an arbitrary configuration [23], and thus realize one-way quantum computation. Accompanied with some local single-qubit measurements, it is sufficient for simulating any arbitrary quantum logic operations. Therefore, experimental or intrinsic difficulties in performing two-qubit operations can be substituted with (possibly probabilistic) generation of a cluster state.

VI. SUMMARY

In conclusion, we describe a scheme to build quantum computers. Both strict strong coupling condition and Lamb-Dicke limit are no longer required. Thus it has high experimental feasibility based on current laboratory technique. By combining etched waveguides and atom traps, toroidal microcavities on a chip are expected to be a *quantum chip* in

the future. One can validate the theory by easily realizing an atom-photon phase gate which is elementary in our scheme. In order to do this, the experimental difficulty can be further reduced. The single photon can be replaced by a weak coherent light pulse which just slightly decreases gate fidelity, and the single atom also can be replaced by multiatoms (CPF gate between single photon and multiatom [29]) which even improve the fidelity.

ACKNOWLEDGMENTS

The authors acknowledge the fruitful discussions with Dr. XiangFa Zhou. This work was funded by the Chinese National Fundamental Research Program (Grant No. 2001CB309301), the Innovation funds from Chinese Academy of Sciences, and National Natural Science Foundation of China (Grant No. 60121503).

[1] A roadmap for quantum information science and technology can be found at http://qist.lanl.gov/
[2] For a review, H. Mabuchi and A. C. Doherty, Science **298**, 1372 (2002) and references therein.
[3] S. B. Zheng and G. C. Guo, Phys. Rev. Lett. **85**, 2392 (2000).
[4] A. Serafini, S. Mancini, and S. Bose, Phys. Rev. Lett. **96**, 010503 (2006).
[5] Y. L. Lim, S. D. Barrett, A. Beige, P. Kok, and L. C. Kwek, Phys. Rev. A **73**, 012304 (2006). Y. L. Lim, A. Beige, and L. C. Kwek, Phys. Rev. Lett. **95**, 030505 (2005).
[6] J. R. Buck, Ph.D. thesis, CIT, 2003.
[7] P. E. Barclay, K. Srinivasan, and O. Painter, Opt. Express **13**, 801 (2005).
[8] V. B. Braginsky and V. S. Ilchenko, Sov. Phys. Dokl., **32**, 307 (1987).
[9] For a review, see K. J. Vahala, Nature (London) **424**, 839 (2003).
[10] J. R. Buck and H. J. Kimble, Phys. Rev. A, **67**, 033806 (2003).
[11] W. Yao, R. Liu, and L. J. Sham, Phys. Rev. Lett., **92**, 217402 (2004); **95**, 030504 (2005).
[12] D. K. Armani, T. J. Kippenberg, S. M. Spillane, and K. J. Vahala, Nature (London) **421**, 925 (2003).
[13] S. M. Spillane, T. J. Kippenberg, K. J. Vahala, K. W. Goh, E. Wilcut, and H. J. Kimble, Phys. Rev. A **71**, 013817 (2005).
[14] D. W. Vernooy and H. J. Kimble, Phys. Rev. A **55**, 1239 (1997).
[15] C. W. Gardiner, and P. Zoller, *Quantum Noise* (Springer-Verlag, Berlin, 1999).
[16] A. S. Sorensen and K. Molmer, Phys. Rev. Lett. **90**, 127903 (2003).
[17] X. F. Zhou, Y. S. Zhang, and G. C. Guo, Phys. Rev. A **71**, 064302 (2005).
[18] H. Rokhsari and K. J. Vahala, Phys. Rev. Lett. **92**, 253905 (2004); M. Cai, O. Painter, and K. J. Vahala, *ibid.* **85**, 74 (2000). S. M. Spillane, T. J. Kippenberg, O. J. Painter, and K. J. Vahala, *ibid.* **91**, 043902 (2003).
[19] H. J. Kimble, in *Cavity Quantum Electrodynamics*, edited by P. R. Berman (Academic, Boston, 1994), pp. 203–267.
[20] Y. F. Xiao, X. M. Lin, J. Gao, Y. Yang, Z. F. Han, and G. C. Guo, Phys. Rev. A **70**, 042314 (2004); Y.-F. Xiao *et al.*, Phys. Lett. A **330**, 137 (2004).
[21] L. M. Duan and H. J. Kimble, Phys. Rev. Lett. **92**, 127902 (2004); L. M. Duan, B. Wang, and H. J. Kimble, Phys. Rev. A **72**, 032333 (2005).
[22] H. Goto and K. Ichimura, Phys. Rev. A **72**, 054301 (2005).
[23] Jaeyoon Cho and H.-W. Lee, Phys. Rev. Lett. **95**, 160501 (2005).
[24] P. Koonath, T. Indukuri, and B. Jalalib, Appl. Phys. Lett. **86**, 091102 (2005).
[25] V. R. Almeida, C. A. Barrios, R. R. Panepucci, and M. Lipson, Nature (London), **431**, 1081 (2004).
[26] J.-C. Tsai, S. Huang, D. Hah, H. Toshiyoshi, and M. C. Wu, IEEE Photonics Technol. Lett. **16**, 1041 (2004).
[27] D. Schrader, I. Dotsenko, M. Khudaverdyan, Y. Miroshychenko, A. Rauschenbeutel, and D. Meschede, Phys. Rev. Lett., **93**, 150501 (2004); S. Kuhr, Science **293**, 278 (2001); W. Hansel, P. Hommelhoff, T. W. Hansch, and J. Reichel, Nature (London) **413**, 498 (2001).
[28] Y. S. Park, Andrew K. Cook, and H. Wang (unpublished).
[29] X. M. Lin, Z. W. Zhou, M. Y. Ye, Y. F. Xiao, and G. C. Guo, Phys. Rev. A **73**, 012323 (2006).